

## Adding further complexity to the polybasite structure: The role of Ag in the *B* layer of the -*M2a2b2c* polytype

LUCA BINDI<sup>1,\*</sup> AND SILVIO MENCHETTI<sup>2,3</sup>

<sup>1</sup>Museo di Storia Naturale, Sezione di Mineralogia, Università di Firenze, Via La Pira 4, I-50121 Firenze, Italy

<sup>2</sup>Dipartimento di Scienze della Terra, Università di Firenze, Via La Pira 4, I-50121 Firenze, Italy

<sup>3</sup>C.N.R., Istituto di Geoscienze e Georisorse sezione di Firenze, Via La Pira 4, I-50121 Firenze, Italy

### ABSTRACT

We report data on the composition and crystal structure of the most Ag-rich (15.63 apfu) natural polybasite yet discovered. It shows the -*M2a2b2c* polytype. The crystal studied was found in a sample (mineralogical collection of the Royal Ontario Museum) from Gowganda, Timiskaming District, Ontario, Canada. Electron microprobe analysis yields the formula  $[\text{Ag}_6(\text{Sb}_{1.78}\text{As}_{0.18})_{\Sigma=1.96}\text{S}_7]$   $[\text{Ag}_9(\text{Ag}_{0.63}\text{Cu}_{0.43})_{\Sigma=1.06}\text{S}_4]$ . Lattice parameters are  $a = 26.2625(4)$ ,  $b = 15.1623(5)$ ,  $c = 24.1061(6)$  Å,  $\beta = 90.045(5)^\circ$ ,  $V = 9599.0(4)$  Å<sup>3</sup>. The structure was refined in the space group *C2/c* to  $R = 0.0581$  using 7725 observed reflections [ $I > 2\sigma(I)$ ]. The refinement shows that one of the three structural positions of the *B* module layer usually occupied by Cu is dominated by Ag. Crystal-chemical characteristics are compared with published data on the other members of the pearceite-polybasite group. Some remarks concerning nomenclature are also given.

**Keywords:** Crystal structure, chemical composition, polytype, silver minerals

### INTRODUCTION

The minerals of the pearceite-polybasite group, general formula  $(M_6T_2S_7)(\text{Ag}_9\text{CuS}_4)$ , with  $M = \text{Ag}$ ,  $\text{Cu}$  and  $T = \text{As}$ ,  $\text{Sb}$ , are relatively common in nature. Their crystal structure can be described as the succession, along the *c* axis, of two pseudo-layer modules: a  $(M_6T_2S_7)^{2-}$  *A* module layer and a  $(\text{Ag}_9\text{CuS}_4)^{2+}$  *B* module layer (Bindi et al. 2007a and references therein). From a chemical point of view, the members of this group are generally pure, only containing minor amounts of Bi, Pb, Zn, and Fe. Nonetheless, the recent discovery of three new mineral species belonging to this group [i.e., selenopolybasite (Bindi et al. 2007b), cupropearceite, and cupropolybasite (Bindi et al. 2007c)] expands the range of chemical compositions reported to date.

In the course of a study dealing with the characterization of structurally complex silver-bearing minerals of mineralogical collections from various museums, we recovered a sample of polybasite (polytype -*M2a2b2c*) with the highest Ag content (>15 apfu) and the lowest Cu content (<1 apfu) yet discovered in nature. Till now the chemical range (in atoms per formula unit) for polybasite-*M2a2b2c* samples was 13.62–14.98 for Ag and 1.01–2.42 for Cu (Bindi et al. 2007a; Hall 1967). The occurrence of polybasite samples with Cu content <1.00 apfu gives the possibility for an unusual crystal structure. The current study evaluates the structure of polybasite with such a low Cu content.

### OCCURRENCE AND CHEMICAL COMPOSITION

The sample containing the polybasite crystal used in the present study (Department of Natural History, Royal Ontario Museum, Canada; catalog no. M27183) is from Gowganda, Timiskaming District, Ontario, Canada, a well-known source of

silver-bearing minerals. Geologic and metallogenetic data for this deposit were reported by Andrews et al. (1986).

Polybasite occurs as very rare black anhedral to subhedral grains, up to 150 µm in length, and shows a gray-black to black streak. A preliminary chemical analysis using energy dispersive spectrometry, performed on the crystal fragment used for the structural study, did not indicate the presence of elements ( $Z > 9$ ) other than S, Cu, As, Ag, Sb, and Pb. The chemical composition was then determined using wavelength dispersive analysis (WDS) by means of a JEOL JXA-8200 electron microprobe. Major and minor elements were determined at a 20 kV accelerating voltage and a 40 nA beam current, with 10 s as counting time. For the WDS analyses the following lines were used: SK $\alpha$ , FeK $\alpha$ , CuK $\alpha$ , ZnK $\alpha$ , AsL $\alpha$ , SeL $\alpha$ , AgL $\alpha$ , SbL $\beta$ , TeL $\alpha$ , AuM $\alpha$ , and PbM $\alpha$ . The standards employed include: native elements for Cu, Ag, Au, and Te, galena for Pb; pyrite for Fe and S; synthetic Sb<sub>2</sub>S<sub>3</sub> for Sb; synthetic As<sub>2</sub>S<sub>3</sub> for As; synthetic ZnS for Zn; and synthetic PtSe<sub>2</sub> for Se. The polybasite fragment was found to be homogeneous within analytical error. The average chemical composition (nine analyses on different spots), together with ranges of wt% of elements, are reported in Table 1. On the basis of 29 atoms, the formula can be written as  $[\text{Ag}_6(\text{Sb}_{1.78}\text{As}_{0.18})_{\Sigma=1.96}\text{S}_7]$   $[\text{Ag}_9(\text{Ag}_{0.63}\text{Cu}_{0.43})_{\Sigma=1.06}\text{S}_4]$ .

### X-RAY SINGLE-CRYSTAL DIFFRACTION AND STRUCTURE REFINEMENT

The diffraction quality of the single crystal was initially checked by means of a Bruker P4 single-crystal diffractometer equipped with a conventional point detector. The data collection was then carried out with an Oxford Diffraction Xcalibur 3 diffractometer, equipped with a Sapphire 2 CCD detector (see Table 2 for details). Intensity integration and standard Lorentz-polarization correction were performed with the CrysAlis RED

\* E-mail: luca.bindi@unifi.it

**TABLE 1.** Electron microprobe data (means and ranges in wt% of elements) and atomic ratios (on the basis of 29 atoms) with their standard deviations ( $\sigma$ ) in parentheses for the selected crystal

	Mean	Ranges	Ratios	( $\sigma$ )
Ag	73.25	72.98–73.69	15.63	(0.21)
Cu	1.20	1.15–1.31	0.43	(0.06)
Pb	0.05	0.02–0.07	0.01	(0.01)
Zn	0.00	0.00–0.02	–	
Fe	0.00	0.00–0.02	–	
Au	0.00	0.00–0.01	–	
Sb	9.44	9.10–10.03	1.78	(0.08)
As	0.59	0.24–0.76	0.18	(0.05)
S	15.26	15.11–15.67	10.97	(0.11)
Se	0.00	0.00–0.02	–	
Te	0.02	0.01–0.07	–	
Total	99.81	99.10–100.25	29.00	

**TABLE 2.** Crystallographic data for the selected crystal

<b>Crystal data</b>	
Chemical formula	$\text{Ag}_{15.50}\text{Cu}_{0.50}\text{Sb}_{1.90}\text{As}_{0.10}\text{S}_{11}$
Temperature (K)	300
Space group	$C2/c$ (no. 15)
Cell parameters:	
$a$ (Å)	26.2625(4)
$b$ (Å)	15.1623(5)
$c$ (Å)	24.1061(6)
$\beta$ (°)	90.045(5)
$V$ (Å <sup>3</sup> )	9599.0(4)
$Z$	16
Crystal color	black
Crystal shape	block
Crystal size (mm)	0.06 × 0.09 × 0.14
<b>Data Collection</b>	
Diffractometer	Oxford Diffraction Excalibur 3
Radiation	$\text{MoK}\alpha$ ( $\lambda = 0.71073$ Å)
Monochromator	oriented graphite (002)
Scan mode	$\phi/\omega$
$\sin\theta/\lambda_{\max}$ (Å <sup>-1</sup> ), $\theta_{\max}$ (°)	0.754, 34.79
$hkl$ range	$-41 \leq h \leq 41$ $-23 \leq k \leq 20$ $-38 \leq l \leq 32$
No. of reflections	89707
<b>Data Reduction</b>	
Absorption correction	multi-scan (ABSPACK; Oxford Diffraction 2006)
No. of independent reflections	29768
Criterion for obs.	$I > 2\sigma(I)$
No. of observed reflections	7725
$R_{\text{int}}$	0.0655
<b>Refinement</b>	
Refinement coefficient	$F^2$
No. of refined parameters	443
Weighting scheme	$w = 1/[\sigma^2(I) + (0.044 \times I)^2]$
$R^*$ (obs), $R^*$ (all)	0.0581, 0.1172
$wR^{2*}$ (obs), $wR^{2*}$ (all)	0.0541, 0.0751
$S$ (obs), $S$ (all)	0.73, 1.04
Secondary ext. coeff. †	none
Diff. Fourier (e <sup>-</sup> /Å <sup>3</sup> )	[-2.03, 2.15]

\*  $\sum |F_o| - |F_c| / \sum |F_o| \cdot wR^2 = [\sum w(|F_o|^2 - |F_c|^2)^2 / \sum w(|F_o|^4)]^{1/2}$ .

† Isotropic secondary extinction: Type I – Gaussian distribution (Becker and Coppens 1974).

(Oxford Diffraction 2006) software package. The program ABSPACK in CrysAlis RED (Oxford Diffraction 2006) was used for the absorption correction.

The program JANA2000 (Petříček et al. 2000) was used for the refinement of the structure, which was carried out in the space group  $C2/c$  starting from the atomic coordinates given by Evain et al. (2006) for the crystal structure of polybasite-*M2a2b2c*. Site-scattering values were refined using scattering curves (Ibers and

Hamilton 1974) for neutral species for the Sb sites (Sb vs. As) and for the Cu sites (Ag vs. Cu) of the *B* module layer (hereafter labeled B sites). One of the B sites (i.e., B3) was found to be fully occupied by Ag. The site-scattering values obtained were fixed during subsequent refinement cycles. With the introduction of twinning by metric merohedry the refinement smoothly converged to  $R = 0.142$  for observed reflections [ $I > 2\sigma(I)$ ], including all the collected reflections in the refinement. Indeed, the peculiar geometry of the pseudo-orthorhombic unit cell (with  $a \approx 3^{1/2} b$ ) makes a {110} twinning very probable. Based on this refinement, the analyses of the difference Fourier synthesis maps suggested an additional twin law with a twofold axis, perpendicular to the previous threefold axis as a generator twin element, thus leading to a second-degree twin. The introduction of only three new parameters (the new twin volume ratios) dramatically lowered the  $R$  value to 0.082, although the new domains were rather small in size [3.38(5), 2.98(3), and 2.12(5)%].

A non-harmonic approach with a Gram-Charlier development of the Debye-Waller factor up to the third order (Johnson and Levy 1974; Kuhs 1984) was then used to describe the electron density in the vicinity of four Ag atoms (i.e., Ag15, Ag22, Ag24, Ag29) for which residues were found in the difference-Fourier synthesis maps. Using this approach, with anisotropic atomic displacement parameters for all the metals but Sb atoms and no constraints, the residual value settled at  $R = 0.0581$  ( $R_w = 0.0541$ ) for 7725 independent observed reflections [ $I > 2\sigma(I)$ ] and 443 parameters, and at  $R = 0.1172$  ( $R_w = 0.0751$ ) for all 29768 independent reflections. Atomic parameters are reported in Tables 3 to 5. Bond distances are reported in Table 6. Table 7<sup>1</sup> lists the observed and calculated structure factors. Bond-valence sums calculated from the curves of Brese and O'Keeffe (1991) are reported in Table 8.

## RESULTS AND DISCUSSION

As already described in the previous structural studies (Bindi et al. 2007a and references therein), the crystal structure of polybasite-*M2a2b2c* (Fig. 1) can be seen as a succession along the *c*-axis of two module layers: the  $[(\text{Ag},\text{Cu})_6\text{Sb}_2\text{S}_7]^{2-} A$  (or  $A'$ ) module layer and the  $[\text{Ag}_9\text{CuS}_4]^{2+} B$  (or  $B'$ ) module layer ( $A,B$  and  $A',B'$  being related by a *c* glide mirror symmetry operation).

In the  $[(\text{Ag},\text{Cu})_6\text{Sb}_2\text{S}_7]^{2-} A$  (or  $A'$ ) module layer, each Ag cation has threefold coordination with sulfur. The (Sb,As) atoms are in threefold coordination occupying the top of a trigonal pyramid with the three S atoms forming a base. The overall mean bond distance for the four structural positions (Sb,As) of 2.42 Å is consistent with the value obtained by considering the  $\langle \text{As}-\text{S} \rangle$  and the  $\langle \text{Sb}-\text{S} \rangle$  bonds of pure pyrargyrite,  $\text{Ag}_3(\text{Sb}_3)$ , and proustite,  $\text{Ag}_3(\text{AsS}_3)$ , [2.452 and 2.293 Å, respectively, Engel and Nowacki (1966)]. Taking into account the molar fractions

<sup>1</sup> Deposit item AM-09-001, Table 7 and CIF. Deposit items are available two ways: For a paper copy contact the Business Office of the Mineralogical Society of America (see inside front cover of recent issue) for price information. For an electronic copy visit the MSA web site at <http://www.minsocam.org>, go to the American Mineralogist Contents, find the table of contents for the specific volume/issue wanted, and then click on the deposit link there.

**TABLE 3.** Site occupancy factors, fractional atomic coordinates, and equivalent isotropic displacement parameters ( $\text{\AA}^2$ ) for the selected crystal

Atom	s.o.f.	x	y	z	$U_{\text{eq}}$
Sb1	1	0.16697(7)	0.24560(10)	0.04547(6)	0.0255(5)
Sb2	0.940(4)	0.16603(6)	0.75682(11)	0.04761(7)	0.0248(5)
As2	0.060	0.16603	0.75682	0.04761	0.0248
Sb3	0.887(4)	0.42090(5)	-0.00620(10)	0.04553(7)	0.0211(5)
As3	0.113	0.42090	-0.00620	0.04553	0.0211
Sb4	0.970(5)	0.41117(6)	0.50116(10)	0.04664(7)	0.0230(4)
As4	0.030	0.41117	0.50116	0.04664	0.0230
Ag1	1	0.03327(7)	0.14640(13)	0.05460(10)	0.0383(7)
Ag2	1	0.04445(8)	0.36054(16)	0.06736(11)	0.0550(9)
Ag3	1	0.04223(9)	0.63232(17)	0.06985(12)	0.0645(10)
Ag4	1	0.03034(9)	0.86010(16)	0.05625(11)	0.0554(9)
Ag5	1	0.16433(9)	0.00350(13)	0.07374(10)	0.0525(7)
Ag6	1	0.18503(7)	0.50161(14)	0.05040(9)	0.0384(6)
Ag7	1	0.28760(9)	0.10213(16)	0.05265(11)	0.0489(8)
Ag8	1	0.28421(8)	0.37824(13)	0.06417(10)	0.0405(7)
Ag9	1	0.28850(10)	0.62833(16)	0.06437(12)	0.0640(10)
Ag10	1	0.28749(7)	0.89934(13)	0.05738(10)	0.0343(7)
Ag11	1	0.43058(9)	0.25118(14)	0.05742(12)	0.0497(9)
Ag12	1	0.41698(12)	0.74589(14)	0.06314(13)	0.0674(11)
Ag13	1	0.16001(7)	0.00609(16)	0.19907(10)	0.0515(8)
Ag14	1	0.34452(9)	0.0312(3)	0.18207(12)	0.1040(16)
Ag15	1	0.46082(16)	0.0105(3)	0.19473(19)	0.0641(10)
Ag16	1	0.09767(9)	0.19270(17)	0.19874(11)	0.0614(9)
Ag17	1	0.22634(9)	0.17236(14)	0.19506(10)	0.0515(8)
Ag18	1	0.41210(8)	0.2091(2)	0.18771(11)	0.0686(11)
Ag19	1	0.05189(9)	0.37802(12)	0.19629(10)	0.0455(8)
Ag20	1	0.17386(9)	0.37652(15)	0.19196(10)	0.0514(8)
Ag21	1	0.29023(9)	0.36011(14)	0.19436(10)	0.0546(8)
Ag22	1	0.40168(17)	0.4163(3)	0.19268(18)	0.0692(11)
Ag23	1	0.06027(10)	0.63451(15)	0.19421(13)	0.0734(11)
Ag24	1	0.1883(2)	0.6293(3)	0.18616(18)	0.0803(11)
Ag25	1	0.31375(13)	0.60684(20)	0.19060(11)	0.0904(12)
Ag26	1	0.46793(13)	0.59306(18)	0.18465(11)	0.0878(13)
Ag27	1	0.02228(10)	0.90307(16)	0.18651(11)	0.0703(10)
Ag28	1	0.13263(12)	0.80886(16)	0.19465(11)	0.0755(11)
Ag29	1	0.2613(3)	0.8440(3)	0.1924(2)	0.1089(15)
Ag30	1	0.41349(8)	0.8008(2)	0.18820(10)	0.0677(10)
B1 (Cu)	1	0	0.2422(3)	0.25	0.0258(13)
B2 (Cu)	1	0	0.7547(4)	0.25	0.057(2)
B3 (Ag)	1	0.24397(9)	0.50475(18)	0.24931(13)	0.0247(8)
S1	1	0.1190(2)	0.1408(4)	0.0977(3)	0.0284(14)
S2	1	0.1341(2)	0.3762(4)	0.0927(3)	0.0259(14)
S3	1	0.2463(2)	0.2349(3)	0.0964(3)	0.0222(12)
S4	1	0.1351(2)	0.6280(4)	0.0930(3)	0.0234(13)
S5	1	0.11961(19)	0.8635(3)	0.1033(2)	0.0210(12)
S6	1	0.2454(2)	0.7580(4)	0.0969(3)	0.0246(13)
S7	1	0.4974(2)	-0.0055(4)	0.1036(2)	0.0251(12)
S8	1	0.3777(2)	0.1178(4)	0.0885(3)	0.0233(13)
S9	1	0.3794(2)	0.3746(4)	0.0957(3)	0.0264(13)
S10	1	0.49517(20)	0.5019(4)	0.0873(3)	0.0265(13)
S11	1	0.37779(18)	0.6152(3)	0.1086(2)	0.0179(11)
S12	1	0.3747(2)	0.8860(4)	0.0984(3)	0.0234(13)
S13	1	0.22953(18)	-0.0051(4)	-0.0002(3)	0.0308(13)
S14	1	0.4906(2)	0.7734(4)	0.0009(3)	0.0470(18)
S15	1	0.0743(2)	0.0162(4)	0.2328(3)	0.0280(13)
S16	1	0.2478(2)	0.0036(4)	0.1527(3)	0.0274(13)
S17	1	0.0024(2)	0.2555(4)	0.1610(2)	0.0205(11)
S18	1	0.3287(2)	0.2261(4)	0.2314(3)	0.0301(14)
S19	1	0.1004(2)	0.5042(4)	0.2324(2)	0.0296(13)
S20	1	0.24750(20)	0.4936(4)	0.1498(3)	0.0232(12)
S21	1	0.0006(3)	0.7404(4)	0.1610(3)	0.0353(14)
S22	1	0.3318(2)	0.7536(4)	0.23534(19)	0.0214(10)

**FIGURE 1.** Projection of the polybasite-*M2a2b2c* structure along the monoclinic *b* axis, emphasizing the succession of the  $[(\text{Ag}, \text{Cu})_6\text{Sb}_2\text{S}_7]^{2-}$  *A* (*A'*) and  $[\text{Ag}_9\text{Cu}_4]^{2+}$  *B* (*B'*) module layers. Light gray, black, and white circles indicate Ag, Sb, and S atoms, respectively. Dark gray circles indicate B1 and B2 positions (Cu atoms), whereas B3 (Ag atoms) is indicated with white circles with dots. The unit-cell is outlined. *A*, *B* and *A'*, *B'* are related by a *c* glide mirror symmetry operation.**TABLE 4.** Anisotropic displacement parameters  $U_{ij}$  ( $\text{\AA}^2$ ) for the selected crystal

Atom	$U_{11}$	$U_{22}$	$U_{33}$	$U_{12}$	$U_{13}$	$U_{23}$
Ag1	0.0327(11)	0.0311(10)	0.0511(15)	-0.0065(8)	-0.0123(11)	0.0081(11)
Ag2	0.0274(11)	0.0634(15)	0.0743(19)	-0.0031(10)	-0.0097(12)	0.0071(14)
Ag3	0.0484(15)	0.0687(17)	0.076(2)	-0.0276(12)	-0.0101(14)	0.0311(15)
Ag4	0.0513(14)	0.0525(15)	0.0624(19)	0.0041(11)	-0.0018(13)	-0.0060(14)
Ag5	0.0753(14)	0.0280(10)	0.0542(14)	-0.0011(11)	0.0293(12)	-0.0023(12)
Ag6	0.0372(10)	0.0391(10)	0.0390(12)	-0.0040(9)	0.0112(9)	0.0030(12)
Ag7	0.0515(14)	0.0478(13)	0.0475(16)	0.0004(11)	0.0029(12)	-0.0067(12)
Ag8	0.0362(12)	0.0360(12)	0.0494(15)	-0.0077(9)	0.0002(11)	0.0014(11)
Ag9	0.0640(17)	0.0559(16)	0.072(2)	0.0245(13)	-0.0021(15)	-0.0133(15)
Ag10	0.0236(10)	0.0278(9)	0.0513(14)	-0.0063(7)	-0.0092(10)	0.0101(10)
Ag11	0.0413(12)	0.0409(12)	0.067(2)	-0.0061(9)	0.0016(13)	0.0033(12)
Ag12	0.109(2)	0.0323(12)	0.061(2)	-0.0095(12)	0.0169(17)	0.0098(12)
Ag13	0.0268(10)	0.0743(15)	0.0535(14)	0.0005(11)	0.0036(10)	-0.0153(14)
Ag14	0.0408(14)	0.223(4)	0.0485(18)	-0.0255(19)	-0.0032(13)	0.006(2)
Ag15	0.0568(14)	0.092(2)	0.0437(14)	0.0092(15)	0.0127(12)	0.0015(17)
Ag16	0.0560(15)	0.0755(16)	0.0528(16)	0.0193(12)	-0.0144(13)	-0.0256(14)
Ag17	0.0667(15)	0.0464(13)	0.0415(14)	0.0057(10)	0.0154(12)	-0.0053(11)
Ag18	0.0318(12)	0.115(2)	0.0588(18)	0.0029(13)	0.0036(13)	0.0330(18)
Ag19	0.0620(14)	0.0216(10)	0.0528(16)	-0.0164(9)	-0.0211(12)	0.0031(10)
Ag20	0.0617(15)	0.0601(15)	0.0323(13)	0.0090(11)	0.0071(12)	0.0135(12)
Ag21	0.0685(16)	0.0437(12)	0.0515(16)	0.0244(11)	0.0083(13)	0.0178(12)
Ag22	0.0766(17)	0.092(2)	0.0393(15)	-0.0418(16)	-0.0024(14)	-0.0208(16)
Ag23	0.0875(19)	0.0481(14)	0.085(2)	0.0251(13)	-0.0434(17)	-0.0158(15)
Ag24	0.129(2)	0.0776(19)	0.0338(15)	0.0762(18)	-0.0018(16)	-0.0053(14)
Ag25	0.149(3)	0.0889(19)	0.0331(15)	-0.0899(19)	0.0244(17)	-0.0138(14)
Ag26	0.169(3)	0.0526(15)	0.0416(16)	-0.0535(17)	-0.0044(19)	0.0075(14)
Ag27	0.0938(19)	0.0523(14)	0.0649(18)	-0.0405(13)	0.0328(16)	-0.0274(14)
Ag28	0.137(2)	0.0508(15)	0.0382(15)	0.0065(16)	-0.0199(17)	0.0105(13)
Ag29	0.212(4)	0.0628(18)	0.0515(19)	0.073(2)	-0.035(2)	-0.0144(16)
Ag30	0.0378(13)	0.128(2)	0.0370(15)	0.0107(14)	-0.0019(12)	0.0083(17)
B1 (Cu)	0.027(2)	0.040(2)	0.0106(19)	0	0.003(2)	0
B2 (Cu)	0.083(4)	0.048(3)	0.041(3)	0	0.005(4)	0
B3 (Ag)	0.0361(15)	0.0259(15)	0.0121(11)	0.0024(12)	-0.0038(14)	0.0013(14)

Note: Third-order tensor elements  $C^{ijk}$  are multiplied by  $10^3$ .

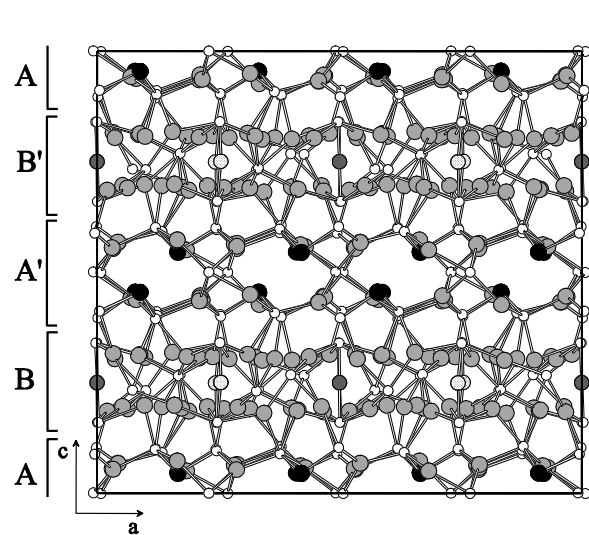


**TABLE 6.** Main interatomic distances ( $\text{\AA}$ ) for the selected crystal

$[(\text{Ag}, \text{Cu})_8(\text{As}, \text{Sb})_2]^{2-} \text{A} (\text{A}') \text{ layer}$					
Sb1-S2	2.443(6)	Sb2-S4	2.382(6)		
Sb1-S1	2.388(6)	Sb2-S5	2.431(6)		
Sb1-S3	2.424(6)	Sb2-S6	2.399(6)		
$\langle \text{Sb1-S} \rangle$	2.418	$\langle \text{Sb2-S} \rangle$	2.404		
Sb3-S8	2.428(6)	Sb4-S11	2.449(5)		
Sb3-S12	2.402(6)	Sb4-S9	2.403(6)		
Sb3-S7	2.450(6)	Sb4-S10	2.413(6)		
$\langle \text{Sb3-S} \rangle$	2.427	$\langle \text{Sb4-S} \rangle$	2.422		
Ag1-S1	2.481(6)	Ag2-S2	2.442(6)	Ag3-S14	2.385(8)
Ag1-S10	2.534(6)	Ag2-S14	2.512(8)	Ag3-S7	2.532(6)
Ag1-S14	2.577(7)	Ag2-S7	2.533(6)	Ag3-S4	2.502(6)
$\langle \text{Ag1-S} \rangle$	2.531	$\langle \text{Ag2-S} \rangle$	2.496	$\langle \text{Ag3-S} \rangle$	2.473
Ag4-S14	2.509(8)	Ag5-S1	2.467(6)	Ag6-S2	2.539(6)
Ag4-S10	2.457(6)	Ag5-S13	2.476(6)	Ag6-S13	2.550(6)
Ag4-S5	2.604(6)	Ag5-S5	2.529(6)	Ag6-S4	2.540(6)
$\langle \text{Ag4-S} \rangle$	2.523	$\langle \text{Ag5-S} \rangle$	2.491	$\langle \text{Ag6-S} \rangle$	2.543
Ag7-S8	2.530(6)	Ag8-S3	2.513(6)	Ag9-S6	2.400(6)
Ag7-S13	2.568(6)	Ag8-S13	2.491(7)	Ag9-S13	2.470(7)
Ag7-S3	2.519(6)	Ag8-S9	2.612(6)	Ag9-S11	2.583(6)
$\langle \text{Ag7-S} \rangle$	2.539	$\langle \text{Ag8-S} \rangle$	2.539	$\langle \text{Ag9-S} \rangle$	2.484
Ag10-S12	2.503(6)	Ag11-S14	2.530(7)	Ag12-S14	2.484(8)
Ag10-S13	2.518(6)	Ag11-S9	2.483(6)	Ag12-S11	2.488(6)
Ag10-S6	2.592(6)	Ag11-S8	2.565(6)	Ag12-S12	2.544(6)
$\langle \text{Ag10-S} \rangle$	2.538	$\langle \text{Ag11-S} \rangle$	2.526	$\langle \text{Ag12-S} \rangle$	2.505
$[\text{Ag}_9\text{CuS}_4]^{2+} \text{B} (\text{B}') \text{ layer}$					
B1-S17	2.156(5)	B2-S21	2.157(6)	B3-S20	2.405(7)
B1-S17	2.156(5)	B2-S21	2.157(6)	B3-S16	2.371(7)
$\langle \text{B1-S} \rangle$	2.156	$\langle \text{B2-S} \rangle$	2.157	$\langle \text{B3-S} \rangle$	2.388
Ag22-S15	2.433(8)	Ag13-S15	2.399(6)	Ag15-S19	2.383(7)
Ag22-S9	2.491(8)	Ag13-S16	2.562(6)	Ag15-S7	2.410(7)
$\langle \text{Ag22-S} \rangle$	2.462	$\langle \text{Ag13-S} \rangle$	2.481	$\langle \text{Ag15-S} \rangle$	2.397
Ag28-S18	2.405(7)	Ag21-S18	2.437(6)	Ag19-S17	2.422(6)
Ag28-S5	2.377(6)	Ag21-S20	2.551(6)	Ag19-S19	2.457(6)
$\langle \text{Ag28-S} \rangle$	2.391	$\langle \text{Ag21-S} \rangle$	2.494	$\langle \text{Ag19-S} \rangle$	2.440
Ag23-S19	2.421(6)	Ag18-S18	2.445(6)	Ag27-S15	2.460(6)
Ag23-S21	2.383(7)	Ag18-S21	2.458(7)	Ag27-S21	2.605(7)
$\langle \text{Ag23-S} \rangle$	2.402	$\langle \text{Ag18-S} \rangle$	2.907(7)	Ag27-S10	2.911(7)
		$\langle \text{Ag22-S} \rangle$	2.603	$\langle \text{Ag22-S} \rangle$	2.659
Ag30-S22	2.531(6)	Ag25-S22	2.518(6)	Ag29-S22	2.526(9)
Ag30-S17	2.520(6)	Ag25-S20	2.634(6)	Ag29-S16	2.625(8)
Ag30-S12	2.718(6)	Ag25-S11	2.599(6)	Ag29-S6	2.678(8)
$\langle \text{Ag30-S} \rangle$	2.590	$\langle \text{Ag25-S} \rangle$	2.584	$\langle \text{Ag29-S} \rangle$	2.610
Ag24-S18	2.512(8)	Ag17-S22	2.583(6)	Ag20-S22	2.562(6)
Ag24-S20	2.723(7)	Ag17-S3	2.614(7)	Ag20-S2	2.611(7)
Ag24-S4	2.645(8)	Ag17-S16	2.812(7)	Ag20-S20	2.815(6)
$\langle \text{Ag24-S} \rangle$	2.627	$\langle \text{Ag17-S} \rangle$	2.941(6)	Ag20-S19	2.903(6)
		$\langle \text{Ag17-S} \rangle$	2.738	$\langle \text{Ag20-S} \rangle$	2.723
Ag16-S22	2.608(6)	Ag26-S15	2.560(7)	Ag14-S19	2.550(6)
Ag16-S1	2.620(7)	Ag26-S17	2.684(6)	Ag14-S16	2.670(6)
Ag16-S17	2.827(6)	Ag26-S10	2.817(7)	Ag14-S8	2.753(7)
Ag16-S15	2.866(6)	$\langle \text{Ag26-S} \rangle$	2.687	$\langle \text{Ag14-S} \rangle$	2.658
$\langle \text{Ag16-S} \rangle$	2.730				

of Sb and As obtained by the occupancy refinement (i.e., Sb = 0.95 and As = 0.05 apfu) and the mean bond distances for the pure components, we obtain a value of 2.44  $\text{\AA}$ .

In the  $(\text{Ag}_9\text{CuS}_4)^{2+}$  *B* (or *B'*) module layer, the 18 independent Ag atoms adopt various coordinations extending from quasi linear to quasi tetrahedral (Table 6). The most interesting feature observed in the structure of the polybasite crystal studied here is related, however, to the presence of Ag in the B3 structural position of the *B* module layer. The B positions [B1, B2 (multiplicity and Wyckoff letter: 4e), and B3 (multiplicity and Wyckoff letter: 8f)] are generally occupied by Cu only and exhibit a nearly perfect linear coordination. In the sample studied here, B1 and B2 are occupied by Cu and show bond distances in the range

**TABLE 8.** Bond-valence (v.u.) arrangement for the selected crystal

Atom	BV	Atom	BV
Sb1	3.27(3)	Ag27	0.85(1)
Sb2	3.32(3)	Ag28	1.04(1)
Sb3	3.06(3)	Ag29	0.89(1)
Sb4	3.20(3)	Ag30	0.94(1)
Ag1	1.07(1)	B1 (Cu)	0.91(1)
Ag2	1.28(1)	B2 (Cu)	0.90(1)
Ag3	1.38(2)	B3 (Ag)	1.05(1)
Ag4	1.11(1)	S1	2.30(2)
Ag5	1.33(1)	S2	2.11(2)
Ag6	1.16(1)	S3	2.10(2)
Ag7	1.05(1)	S4	2.18(2)
Ag8	1.20(1)	S5	2.23(2)
Ag9	1.23(1)	S6	2.17(2)
Ag10	1.16(1)	S7	2.17(2)
Ag11	1.08(1)	S8	2.03(2)
Ag12	1.15(1)	S9	2.21(2)
Ag13	0.85(1)	S10	2.18(2)
Ag14	0.79(1)	S11	2.00(2)
Ag15	1.02(2)	S12	2.04(2)
Ag16	0.87(1)	S13	2.26(2)
Ag17	0.88(1)	S14	2.37(2)
Ag18	1.01(1)	S15	1.89(2)
Ag19	0.91(1)	S16	1.80(2)
Ag20	0.91(1)	S17	1.81(1)
Ag21	0.80(1)	S18	1.91(2)
Ag22	0.87(1)	S19	1.92(2)
Ag23	1.02(2)	S20	1.78(1)
Ag24	0.85(1)	S21	1.83(2)
Ag25	0.94(1)	S22	2.01(2)
Ag26	0.74(1)		

Note: Calculated from the bond-valence curves of Brese and O'Keeffe (1991).

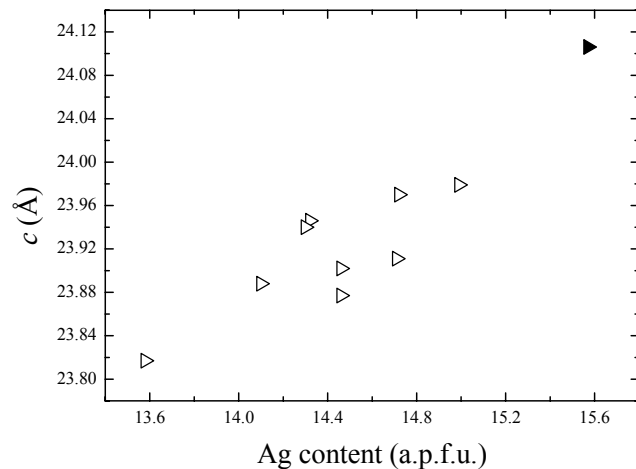


**FIGURE 2.** Relationship between the *c* parameter and the Ag content obtained by electron microprobe for different samples of polybasite-*M2a2b2c*. Empty triangles refer to data taken from Bindi et al. (2007a); solid triangle refers to the M27183 polybasite studied here.

2.156–2.157  $\text{\AA}$ , whereas B3 (fully occupied by Ag) shows a larger mean bond distance of 2.388  $\text{\AA}$ . This value is very close to those observed for the linearly coordinated Ag atoms of the *B* module layer (i.e., Ag13, Ag15, Ag19, Ag21, Ag22, Ag23, Ag28; Table 6). All the B-S bond distances are mainly lined along the *c* axis (Fig. 1). This means that when Ag substitutes for Cu in one of these structural positions we should observe an increase in the *c* lattice parameter and a consequent increase in the volume of the unit cell. Such an increase in cell volume for the Ag-rich polybasite studied here is observed. The unit-cell volume (9599  $\text{\AA}^3$ ) exceeds by far the range of values reported in the literature

►FIGURE 3. Relationship between the unit-cell volume of the hexagonal subcell and the Cu content obtained by electron microprobe for the different members of the pearceite-polybasite group. The equation of the regression line is  $V (\text{\AA}^3) = 607(1) - 12.1(8) \text{ Cu}_{\text{EPMA}} (\text{apfu})$ .

(9242–9504  $\text{\AA}^3$ ; Bindi et al. 2007a). The increase in the unit-cell volume is principally related to the increase in the length of the *c* axis, which is 24.1061  $\text{\AA}$  in the present sample (Fig. 2).

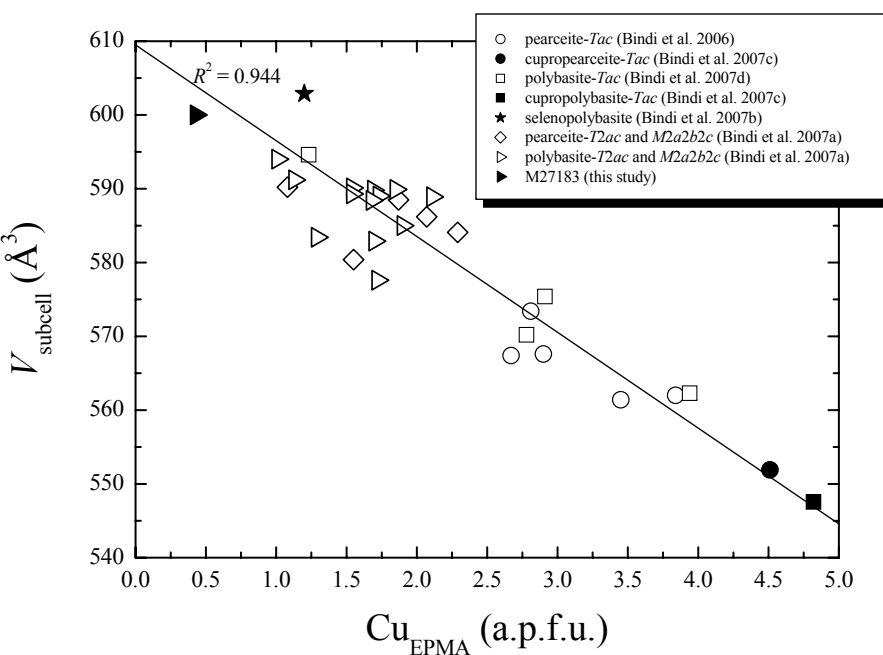
In Figure 3, the variation in unit-cell volume is reported as a function of the Cu content obtained by electron microprobe. To compare all the members belonging to the pearceite-polybasite group, the variation of the hexagonal subcell volume (i.e.,  $a \approx 7.5$ ,  $c \approx 12$   $\text{\AA}$ ) was considered. The polybasite-*M2a2b2c* studied here (black triangle in Fig. 3) well fits the general trend observed for the minerals of the pearceite-polybasite group and corroborates the findings of Bindi et al. (2007a) that the unit-cell volumes are strongly influenced by the Ag content, whereas the influence of the Sb content is minor.

#### NOMENCLATURE REMARKS

The structural and chemical data reported in this paper for the Ag-rich polybasite-*M2a2b2c* raise the possibility that the mineral deserves its own name. Indeed, if we take into account the rule that a mineral could be considered as new when a structural site is dominated by a different cation, then the M27183 polybasite studied here should be regarded a new mineral species (i.e., Ag replacing Cu in the B3 structural position). However, if we write the ideal chemical formula of the M27183 polybasite according to the criteria introduced by Bindi et al. (2007a), it would be  $[\text{Ag}_6\text{Sb}_2\text{S}_7][\text{Ag}_9(\text{Ag}_{0.50}\text{Cu}_{0.50})\text{S}_4]$ . Hence, we do not have a dominance of Ag in the <B1,B2,B3> structural sites of the *B* module layer. The only way to write the formula to explain what was found by the structural analysis is with a doubled formula as  $[\text{Ag}_{12}\text{Sb}_4\text{S}_{14}][\text{Ag}_{18}\text{AgCuS}_8]$ . This way of writing the formula, however, cannot be considered since it would imply another complete reshuffling of names and formulae within this group. Nonetheless, the structural study reported here indicates that the polybasite structure (in the monoclinic polytype) is able to accommodate larger amounts of Ag than recognized previously. This means that it is highly probable that a polybasite-*M2a2b2c* with Ag > Cu in the B sites of the *B* module layer can be found in nature. Such a mineral would be a new mineral species.

#### ACKNOWLEDGMENTS

The authors gratefully acknowledge Paul G. Spry (Iowa State University) for his help in electron microprobe analyses. We thank Robert Ramik (Royal Ontario Museum) who provided us with the polybasite sample. The paper benefited by the official reviews made by Lasse Norén and František Laufek. Associate Editor Diego Gatta is thanked for his efficient handling of the manuscript. This work was funded by CNR, Istituto di Geoscienze e Georisorse, sezione di Firenze and by M.I.U.R., P.R.I.N. 2007, project “Complexity in minerals: modulation, phase transition, structural disorder.”



#### REFERENCES CITED

- Andrews, A.J., Owsiacki, L., Kerrich, R., and Strong, D.F. (1986) The silver deposits at Cobalt and Gowganda, Ontario. I. Geology, petrography, and whole-rock geochemistry. Canadian Journal of Earth Sciences, 23, 1480–1506.
- Becker, P.J. and Coppens, P. (1974) Extinction within the limit of validity of the Darwin transfer equations. I. General formalism for primary and secondary extinction and their applications to spherical crystals. Acta Crystallographica, A30, 129–147.
- Bindi, L., Evain, M., and Menchetti, S. (2006) Temperature dependence of the silver distribution in the crystal structure of natural pearceite,  $(\text{Ag},\text{Cu})_{16}(\text{As},\text{Sb})\text{S}_{11}$ . Acta Crystallographica, B62, 212–219.
- Bindi, L., Evain, M., Spry, P.G., and Menchetti, S. (2007a) The pearceite-polybasite group of minerals: Crystal chemistry and new nomenclature rules. American Mineralogist, 92, 918–925.
- Bindi, L., Evain, M., and Menchetti, S. (2007b) Selenopolybasite,  $[(\text{Ag},\text{Cu})_{16}(\text{Sb},\text{As})(\text{S},\text{Se})_2][\text{Ag}_9\text{Cu}(\text{S},\text{Se})_2\text{Se}_2]$ , a new member of the pearceite-polybasite group from the De Lamar Mine, Owyhee county, Idaho, U.S.A. Canadian Mineralogist, 45, 1525–1528.
- Bindi, L., Evain, M., Spry, P.G., Tait, K.T., and Menchetti, S. (2007c) Structural role of copper in the minerals of the pearceite-polybasite group: the case of the new minerals cupropearceite and cupropolybasite. Mineralogical Magazine, 71, 641–650.
- Bindi, L., Evain, M., and Menchetti, S. (2007d) Complex twinning, polytypism, and disorder phenomena in the crystal structures of antimonpearceite and arsenopolybasite. Canadian Mineralogist, 45, 321–333.
- Brese, N.E. and O’Keeffe, M. (1991) Bond-valence parameters for solids. Acta Crystallographica, B47, 192–197.
- Engel, P. and Nowacki, W. (1966) Die Verfeinerung der Kristallstruktur von Proustit,  $\text{Ag}_3\text{AsS}_3$ , und Pyrargyrit,  $\text{Ag}_3\text{SbS}_3$ . Neues Jahrbuch für Mineralogie Monatshefte, 181–195.
- Evain, M., Bindi, L., and Menchetti, S. (2006) Structural complexity in minerals: Twinning, polytypism, and disorder in the crystal structure of polybasite,  $(\text{Ag},\text{Cu})_{16}(\text{Sb},\text{As})\text{S}_{11}$ . Acta Crystallographica, B62, 447–456.
- Hall, H.T. (1967) The pearceite and polybasite series. American Mineralogist, 52, 1311–1321.
- Ibers, J.A. and Hamilton, W.C. (1974) International Tables for X-ray Crystallography, vol. IV, 366 p. Kynoch Press, Birmingham.
- Johnson, C.K. and Levy, H.A. (1974) Thermal-motion analysis using Bragg diffraction data. In J.A. Ibers and W.C. Hamilton, Eds., International Tables for X-ray Crystallography, vol. IV, p. 311–336. Kynoch Press, Birmingham.
- Kuhs, W.F. (1984) Site-symmetry restrictions on thermal-motion-tensor coefficients up to rank 8. Acta Crystallographica, A40, 133–137.
- Oxford Diffraction (2006) CrysAlis RED (Version 1.171.31.2) and ABSPACK in CrysAlis RED. Oxford Diffraction Ltd., Oxfordshire, England.
- Petříček, V., Dušek, M., and Palatinus, L. (2000) JANA2000, a crystallographic computing system. Institute of Physics, Academy of Sciences of the Czech Republic, Prague.

MANUSCRIPT RECEIVED JUNE 4, 2008

MANUSCRIPT ACCEPTED JULY 10, 2008

MANUSCRIPT HANDLED BY G. DIEGO GATTA